

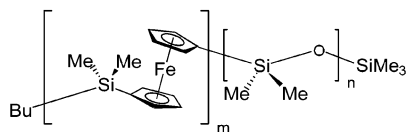
## A Reversible Tube-to-Rod Transition in a Block Copolymer Micelle

Jose Raez, Juan Pablo Tomba, Ian Manners,\* and Mitchell A. Winnik\*

Department of Chemistry, University of Toronto, 80 St. George Street, Toronto, Ontario, Canada M5S 3H6

Received April 23, 2003; E-mail: mwinnik@chem.utoronto.ca

Polyferrocenylsilanes are remarkable polymers. They can be oxidized to a semiconducting state and serve as precursors to magnetic ceramics.<sup>1</sup> Their block copolymers (e.g., those of polyferrocenyldimethylsilane, PFS) form unusual and unexpected self-assembled structures in selective solvents. For example, diblock copolymers of PFS with polyisoprene (PI-*b*-PFS) with a long PI block form dense wormlike micelles in hexane and decane, good solvents for PI but nonsolvents for PFS.<sup>2</sup> In the dry state, these structures can be thought of as self-insulating nanowires in which the rubbery block forms an insulating sheath around the PFS core. When the soluble block is poly(dimethylsiloxane) (PDMS), the type of structure formed depends on the relative lengths of the PFS and PDMS blocks. For example, PFS<sub>50</sub>-PDMS<sub>300</sub> (the subscripts refer to the mean repeat lengths) forms cylindrical (wormlike) micelles in hexane, but when the ratio of PDMS to PFS is increased, the morphology changes.<sup>3</sup> For block ratios of 1:12 and 1:18, long hollow structures are formed.<sup>4,5</sup> While we have only a poor understanding of the factors that control the morphology formed, the characteristic feature of both the tubular and the nanowire structures is a strong peak at ca. 6.4 Å in the wide-angle X-ray scattering pattern, indicative of a (semi)crystalline PFS phase.<sup>3</sup> The PFS homopolymer has a melting range from 120 to 140 °C.<sup>1</sup>



In this Communication, we describe a remarkable morphology transition induced by a change in temperature for a PFS<sub>40</sub>-*b*-PDMS<sub>480</sub> sample in decane solution. This sample, which forms nanotubes at 23 °C, rearranges to form short dense rods when the solution is heated to 50 °C. When the solution is cooled to 25 °C, the system evolves back to nanotubes. Beyond demonstrating a remarkable and unprecedented change in morphology, these experiments demonstrate that both structures are dynamic and represent equilibrium states of the material.

The PFS<sub>40</sub>-*b*-PDMS<sub>480</sub> sample (PDI = 1.01) was synthesized via sequential anionic ring-opening polymerization and purified in a size exclusion column in THF.<sup>4</sup> The copolymer sample was dissolved in *n*-decane at 60 °C and allowed to cool to 25 °C. At this temperature, we observed nanotubes by bright field transmission electron microscopy (TEM, see ref 4 and the inset in Figure 1).<sup>4</sup> These tubes have a width of 20 nm, a wall thickness of ca. 7 nm, and, as reported previously, can have lengths in excess of 10 μm. Thus, the tubes on the TEM grid have a high aspect ratio, with  $p = L/d \gg 10$ . When solutions (ca. 0.33–0.85 mg/mL) are heated at 50 °C and aged for 24 h (time needed for the system to reach equilibrium), we observe dense rods by TEM (Figure 1 and Supporting Information, Figure S1). Samples for TEM were prepared by dipping a carbon-coated copper grid into the warm solution, and also by placing a 20-μL drop onto a coated grid placed

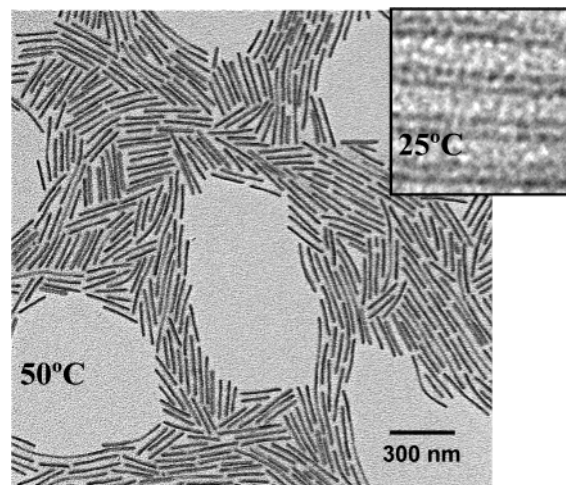


**Figure 1.** TEM micrograph of PFS<sub>40</sub>-*b*-PDMS<sub>480</sub> assemblies formed in *n*-decane at 50 °C. Sample was prepared by dipping a carbon-coated grid into the warm solution. The sample was not stained. The inset (from ref 4) shows nanotubes at 25 °C.

on a piece of filter paper. Either way, we observed the same morphology. Because the PFS block contains Fe, we do not stain the samples, and we take advantage of our sample's natural contrast. Thus, we see only the insoluble PFS domains. The TEM micrograph shows that the PFS cores have diameters ranging from 14 to 20 nm and that most rods have  $p$  values less than 10.

We also characterized the micelle structures in solution using multiangle light-scattering measurements.<sup>6</sup> We are fortunate that the index of refraction of *n*-decane (1.4097 at 25 °C) is virtually identical to that of PDMS ( $n_D$  25 °C = 1.40347). Through fortuitous contrast matching, we are able to probe the insoluble PFS core, while the PDMS corona chains remain “invisible”.

In light-scattering (LS) experiments at low concentrations, the excess Rayleigh ratio,  $\Delta R$ , is related to the sample concentration  $c$ , the second virial coefficient  $A_2$ , and the form factor  $P(q)$  through the expression:

$$\frac{Kc}{\Delta R} = \frac{1}{M_w P(q)} (1 + 2A_2c + \dots) \quad (1)$$

where  $K = 4\pi^2 n_0^2 (dn/dc)^2 / (N_A \lambda^4)$ , and  $N_A$ ,  $\lambda$ ,  $dn/dc$ , and  $n_0$  are Avogadro's number, the incident wavelength (632.8 nm), the refractive index increment (0.0398 mL/g), and the refractive index of the solvent ( $n_D = 1.3987$ ),<sup>8</sup> respectively. Our measured  $dn/dc$  value of PDMS in *n*-decane at 50 °C is  $-6.85 \times 10^{-3}$  mL/g, with an incident wavelength of 620 nm. Data were collected at 26 angles (from 27° to 36°, at 3° intervals, and from 40° to 145° at 5° intervals).

A Zimm plot of the scattering data (Supporting Information, Figure S2) gave an  $M_w$  value of the PFS nanorods of  $1.60 \times 10^6$

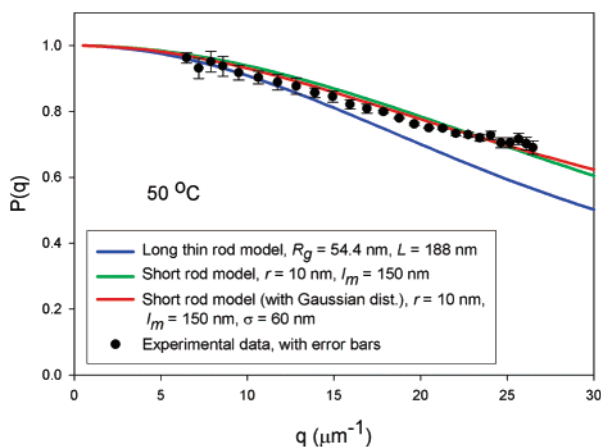


**Figure 2.** Form factor plots comparing the “long-thin” rod model, the “short rigid-rod” model, and “short rigid-rod” model with a Gaussian distribution of rod lengths.

g/mol ( $\pm 0.95\%$ ) with a radius of gyration  $R_g = 54.4$  nm. Because the mass of the PFS block is 9680 g/mol, we calculate an average aggregation number of 165. On the basis of the  $M_w$  of the core, the  $M_w$  of the entire micelle is calculated to be  $7.46 \times 10^6$  g/mol.

To obtain structural information, we extrapolate the scattering intensity to  $c = 0$  and fit the angular dependent scattering intensity to a model. For a “long-thin” rigid rod ( $p \gg 10$ ),  $P(q)_{\text{long}}$  is given by<sup>9</sup>

$$P(q)_{\text{long}} = \frac{2}{qL} \int_0^{qL} \frac{\sin(qL)}{qL} d(qL) - \left( \frac{2}{qL} \sin\left(\frac{qL}{2}\right) \right)^2 \quad (2)$$

where the rod length  $L = 12^{1/2}R_g$ ,  $\theta$  is the scattering angle, and  $q = 4\pi n_{50} \sin(\theta/2)/\lambda$  is the scattering vector.

If a rigid rod has a small aspect ratio,  $P(q)$  is given by<sup>10</sup>

$$P(q)_{\text{short}} = \int_0^{\pi/2} \frac{4 \sin^2(qL/2 \cos \gamma)}{q^2 L^2 \cos^2 \gamma} \frac{4 J_1^2(qr \sin \gamma)}{q^2 r^2 \sin^2 \gamma} \sin \gamma d\gamma \quad (3)$$

where  $r$  is the radial cross section,  $J_1$  is the first-order Bessel function, and  $\gamma$  is the angle between  $q$  and the rod's long axis.

In Figure 2, we show the results of fitting our scattering data to the models described by eqs 2 and 3. For the fit to eq 3, we take advantage of the fact that we see only the PFS core in both the TEM and the LS measurements, and we take the value of the core radius from the TEM images. The data in Figure 2 show that we obtain a poor fit to eq 2, but a reasonable fit to eq 3 (error fit = 0.081%),<sup>11</sup> with an  $L$  value of 150 nm. Varying the radius between 7 and 10 nm did not affect the fit to eq 3. This model, however, does not account for the upturn in the data points in the range of  $q = 20\text{--}27 \mu\text{m}^{-1}$ . To delve deeper into the data analysis, we next consider a Gaussian distribution of rod lengths with a mean length  $l_m$  and a standard deviation ( $\sigma$ ), where the form factor is given by the expression

$$P(q)_{\text{sh,G}} = \int_0^\infty \frac{1}{\sigma\sqrt{2\pi}} \exp\left[-\frac{1}{2}\left(\frac{L-l_m}{\sigma}\right)^2\right] P(q)_{\text{short}} dL \quad (4)$$

With eq 4, the fit is improved significantly, leading to  $l_m = 150$  nm and  $\sigma = 60$  nm (error fit = 0.042%). These lengths are in global

agreement with the values obtained (average  $L = 184$  nm,  $\sigma = 59.4$  nm) from the TEM images using an image analysis program (AIS ver. 6.0). The polydispersity measured from the TEM images is 1.10 ( $L_w/L_n$ ).<sup>12</sup> The concordance between the two sets of values gives us confidence that the objects present in solution correspond to those seen in the TEM image. The small differences in the fitting parameters may point to subtle shortcomings in the model for  $P(q)$ , such as the influence of a distribution of core radii.

When the solution was cooled to 23 °C and allowed to age for a day, the TEM shows that nanotubes were regenerated. The fact that this process can be repeated establishes the dynamic nature of the self-assembled structures and emphasizes that both the tubes and the rods are equilibrium structures. What is less clear are the forces that drive the rearrangement. The theory of coil-crystalline block copolymer micelles primarily predicts a lamellar structure for the crystalline block.<sup>13</sup> A long hollow tube with a fraction of the soluble PDMS chains penetrating into the interior may represent a compromise between the space filling needs of the PDMS coil and a strongly unfavorable edge surface tension of the PFS crystal. Decane is a relatively poor solvent for PDMS at 25 °C, with a Flory–Huggins  $\chi$  value of 0.64.<sup>14</sup> Like analogous  $n$ -alkane solvents,  $n$ -decane is a better solvent for PDMS at higher temperatures.<sup>15</sup> The system can respond to swelling of the PDMS brush by an increase in curvature, leading to the formation of dense rods. The rigidity of the rods is consistent with the semicrystalline nature of the PFS core.

As a hypothesis for future research, we can imagine that the size of the coil formed by the soluble block is a major determinant of whether PFS block copolymers form rods or tubes in selective solvents. Decane is a better solvent for PI than for PDMS. Thus, it may be possible to form tubes of PI-*b*-PFS if a suitable poor solvent for PI can be identified.

**Acknowledgment.** The authors thank NSERC Canada for financial support. J.R. is grateful for an Ontario Graduate Scholarship. We thank Dr. Daniel Portinha, Dr. Christophe Chassenieux (Université Pierre et Marie Curie), and Dr. Pierre Terech (CEA Grenoble, France) for helpful discussions.

**Supporting Information Available:** Experimental details on the light-scattering measurements (PDF). This material is available free of charge via the Internet at <http://pubs.acs.org>.

## References

- (1) Manners, I. *Chem. Commun.* **1999**, 857–865.
- (2) Cao, L.; Manners, I.; Winnik, M. A. *Macromolecules* **2002**, *35*, 8258–8260.
- (3) Massey, J.; Temple, K.; Cao, L.; Rharbi, Y.; Raez, J.; Winnik, M. A.; Manners, I. *J. Am. Chem. Soc.* **2000**, *122*, 11577–11584.
- (4) Raez, J.; Manners, I.; Winnik, M. A. *J. Am. Chem. Soc.* **2002**, *124*, 10381–10395.
- (5) Raez, J.; Manners, I.; Winnik, M. A. *Langmuir* **2002**, *18*, 7229–7239.
- (6) Brown, W. *Light Scattering: Principles and Development*; Clarendon Press: Oxford, 1993.
- (7) *Silicon Compounds: Register & Review*; Petrarch Systems, Inc.: Bristol, 1982; p 172.
- (8) Huglin, M. B. *Light Scattering from Polymer Solutions*; London Academic Press: London, 1972; p 30.
- (9) Debye, P.; Anacker, E. W. *J. Phys. Colloid Chem.* **1951**, *55*, 644–655.
- (10) Mittelbach, P.; Porod, G. *Acta Phys. Austriaca* **1961**, *14*, 185–211.
- (11) The formula for error fit is given in the Supporting Information section.
- (12)  $L_w$  is the weight-average length, and  $L_n$  is the number-average length.
- (13) Vilgis, T.; Halperin, A. *Macromolecules* **1991**, *24*, 2090–2095.
- (14) Hammers, W. E.; Ligny, C. L. *J. Polym. Sci., Polym. Phys. Ed.* **1974**, *12*, 2065–2074.
- (15) Summers, W. R.; Tewari, Y. B.; Schreiber, H. P. *Macromolecules* **1972**, *5*, 12–16; Tian, M.; Munk, P. *J. Chem. Eng. Data* **1994**, *39*, 742–755.

JA030251I